Physics and Imaging in Radiation Oncology 17 (2021) 32–35

Contents lists available at ScienceDirect

Physics and Imaging in Radiation Oncology

journal homepage: www.sciencedirect.com/journal/physics-and-imaging-in-radiation-oncology

Experimental evaluation of four-dimensional Magnetic Resonance Imaging for radiotherapy planning of lung cancer

Terry Perkins [c,d], Danny Lee [b], John Simpson [a,b], Peter Greer [a,b], Jonathan Goodwin [a,b,*]

[a] Radiation Oncology, Calvary Mater Newcastle, Australia
[b] School of Mathematical and Physical Science, University of Newcastle, Australia
[c] Blacktown Cancer & Haematology Centre, Blacktown Hospital, NSW, Australia
[d] School of Physics, University of Sydney, Australia

ARTICLE INFO

Keywords:
4D-MRI
4D-CT
Lung cancer
radial VIBE
Self-navigating

ABSTRACT

Radiotherapy planning for lung cancer typically requires both 3D and 4D Computed Tomography (CT) to account for respiratory related movement. 4D Magnetic Resonance Imaging (MRI) with self-navigation offers a potential alternative with greater reliability in patients with irregular breathing patterns and improved soft tissue contrast. In this study 4D-CT and a 4D-MRI Radial Volumetric Interpolated Breath-hold Examination (VIBE) sequence was evaluated with a 4D phantom and 13 patient respiratory patterns, simulating tumour motion. Quantification of motion related tumour displacement in 4D-MRI and 4D-CT found no statistically significant difference in mean motion range. The results demonstrated the potential viability of 4D-MRI for lung cancer treatment planning.

1. Introduction

Dose escalation in lung cancer radiotherapy is used to potentially improve patient outcomes but can result in increased toxicity to healthy tissue [1]. Achieving effective local tumour control with dose escalation requires accurate determination of tumour extent, spatial distribution and delineation of organs at risk. This process is aided through the use of four dimensional Computed Tomography (4D-CT) [2]. 4D-CT generates multiple 2D images, which are retrospectively sorted into respiratory phase resolved 3D image sets where tumour localisation and extent can be defined [2]. Despite its routine clinical use, 4D-CT is not without limitations, including ionising radiation dose, poor soft tissue contrast, and motion artefacts associated with irregular breathing patterns [3–5].

One of the main advantages Magnetic Resonance Imaging (MRI) offers for oncology applications is superior soft tissue contrast with improved definition of the tumour extent [6]. The recent development of self-navigating gradient echo 4D-MRI sequences such as Radial Volumetric Interpolated Breath-hold Examination (VIBE) sequence means that 4D phase resolved images can be acquired as a potential alternative to 4D-CT for lung cancer treatment planning. Recent work has shown advances in 4D-MRI with improved diagnostic value for moving anatomy [7–10]. This work quantitatively evaluated the extent of motion range measured for a tumour surrogate in a respiratory motion phantom with both 4D radial VIBE MRI and 4D-CT, using a series of pre-recorded patient respiratory patterns.

2. Materials and methods

A 3T MRI scanner (MAGNETOM Skyra, Siemens Healthcare, Erlangen, Germany) and Siemens Somatom Confidence CT scanners (Siemens Healthcare, Erlangen, Germany) were used to acquire 4D image data series. For 4D-MRI, a prototype Siemens Radial VIBE sequence with self-navigating and optional motion correction averaging (mocoAVE) was used. To simulate lung tumour motion, a QUASAR MR-4D phantom (Modus Medical Devices, Ontario Canada) was used during both MR and CT image acquisition. The phantom provides translational and rotational motion of a cylindrical sleeve. The tumour surrogate (plastic sphere) was mounted centrally in the cylinder for superior-inferior motion. Thirteen pre-recorded lung cancer patient breathing patterns obtained during a previous study [11], were used to control the motion of the phantom. The retrospective use of patient data for this study was deemed as a negligible risk and did not require further approval from the Hunter New England Human Research Ethics Committee (Exemption Authorisation AU202012-06).

* Corresponding author.
E-mail address: jonathan.goodwin@newcastle.edu.au (J. Goodwin).

https://doi.org/10.1016/j.phro.2020.12.006
Received 15 June 2020; Received in revised form 18 December 2020; Accepted 22 December 2020
Available online 7 January 2021

2.1. Input respiratory cycle and 4D-CT RPM assessment

The normality of the distribution of respiratory cycle amplitudes for each patient was tested in Matlab (The MathWorks, Natick, PA, USA) using Shapiro-Wilk and Kolmogorov-Smirnov. Median and inter-quartile ranges were used to quantify the variability of input patient respiratory motion. The 95% quantiles of the respiratory input signal trace were used to define motion range as a benchmark for this study to limit the effects of data outliers and be consistent with the literature [12,13]. The effects of baseline drift on 4D-MRI and 4D-CT motion estimation were also investigated, where baseline drift was defined as the maximum to the minimum displacement of a rolling 20 s average of the input respiratory signal trace. To enable the CT respiratory monitoring system (Varian RPM) to work with the phantom, a mechanical device was developed to translate Superior-Inferior motion of the phantom into Anterior-Posterior motion of the RPM marker. To reduce the likelihood of the device being a confounding variable, the raw RPM signal trace was compared to the input respiratory signal trace using Spearman's Rank Correlation.

2.2. MRI self-navigation assessment

Phase binning of MRI raw data was achieved through a self-navigation signal, acquired through repeated sampling of k-space centre during radial acquisition. A time series cross covariance technique was applied to identify the locations within the navigator signal with the highest correlation with the input respiratory trace. The input respiratory trace was then aligned with the locations of highest cross-covariance by applying the appropriate lag to each repetition of the input respiratory trace. Only sections with a full input respiratory cycle were used for further analysis. The self-navigator/respiratory signal Spearman's rank correlation was calculated to show this is not a confounding variable.

As the self-navigation signal relies on the proportion of tissue with high (or low) transverse magnetisation moving in/out of the excited volume during respiration [14], the effect of reducing field of view (FOV) was investigated at two different in plane resolutions (0.52×0.52 mm^2, 1.6×1.6 mm^2), for one shallow respiratory motion pattern where the 380×380 mm^2 FOV was reduced to 150×150 mm^2, in order to focus more closely around the moving tumour surrogate across the respiratory cycle.

2.3. Motion range comparison of 4D-CT, 4D-MRI and the respiratory signal trace

The measured motion ranges from 4D-CT images, 4D-MRI images and the input respiratory signal trace 95% quantiles were compared with a repeated measures ANOVA test to assess if there was a statistically significant difference between the motion ranges. To analyse the data statistically, R-Studio [15] and MATLAB were used. An ad-hoc paired *t*-test was performed between each of the three motion ranges to quantify differences between individual pairs.

3. Results

For 12 of the 13 respiratory patterns, median respiratory amplitude ranged from 10.5 mm to 24.7 mm, respiratory inter-quartile range was 8% to 68% of the median amplitude and baseline drift was between 18% and 104% of median amplitude. The most variable respiratory pattern (patient 12) had a median amplitude of 6.1 mm, respiratory inter-quartile range was 62% of the median amplitude and baseline drift was 167% of median amplitude. Fig. 2 shows the relationship between the amplitude variability, the baseline drift and the measured 4D-CT and 4D-MRI motion ranges. The 4D-CT RPM Spearman's rank correlation average for all 4D-CT data was 0.94 ($p < 0.01$). With a FOV of 380 mm (in plane resolution of 1.32×1.32 mm2), 12 out of the 13 respiratory patterns had a Spearman's Rank correlation of greater than 0.96 ($p < 0.01$).

The reduction in FOV and increase in resolution for the poor performing self-navigation cycle (FOV = 150 mm, pixel 0.52×0.52 mm^2) resulted in the average Spearman's Rank correlation increasing from 0.23 ($p < 0.01$) to 0.97 ($p < 0.01$). A similar observation was made with the same FOV reduction, with a reduced image resolution (Spearman's 0.93 ($p < 0.01$), FOV = 150 mm, pixel 1.6×1.6 mm^2).

Table 1 shows the results of the normality test for the motion range distribution of the 4D-CT, 4D-MRI and the input respiratory signal (Q95%).

Repeated measures ANOVA between 4D-MRI, 4D-CT and input respiratory 95% quantiles gave a test statistic of $F = 0.05$ ($p = 0.95$). The paired *t*-test results between 4D-MRI, 4D-CT and input respiratory 95% quantiles had a p-value $\gg 0.05$ (p-values; MRI-CT = 0.77, MRI-input Q95% = 0.60, CT-input Q95% = 0.68.

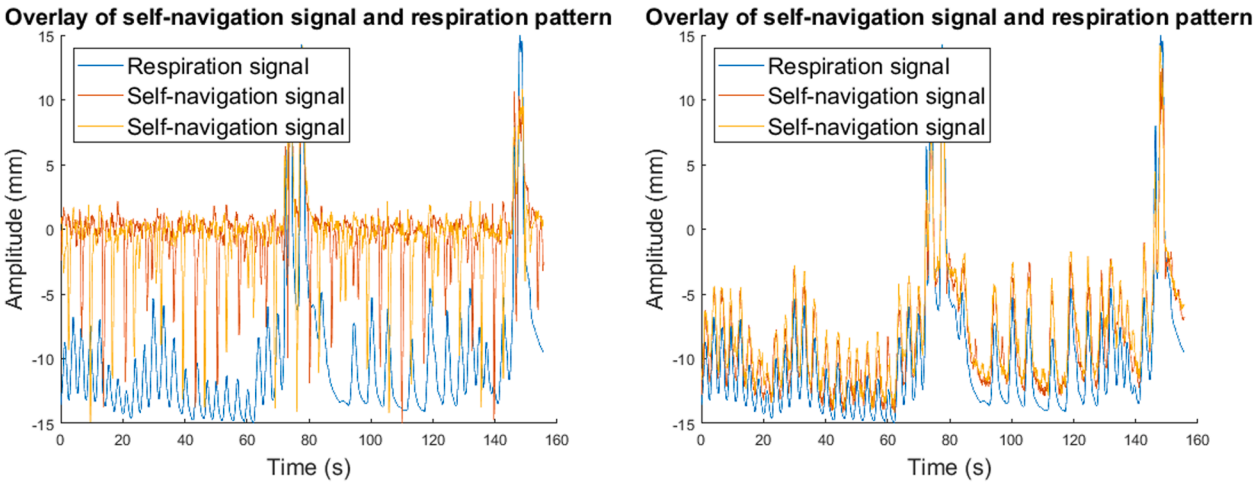

Fig. 1. Patient 12 self-navigation signal overlayed on the input respiratory signal. Left (A); The navigation signal is inverted in this plot. Note the good correlation between the maximum peaks of the pattern and the inverted FID navigation signal. Right (B); Patient 12 respiratory pattern and FID navigation signal when the FOV is reduced from 380 mm to 150 mm. Spearman's Rank correlation improvement 0.23 ($p < 0.01$) Fig. 1(A) to 0.97 ($p < 0.01$) Fig. 1(B).

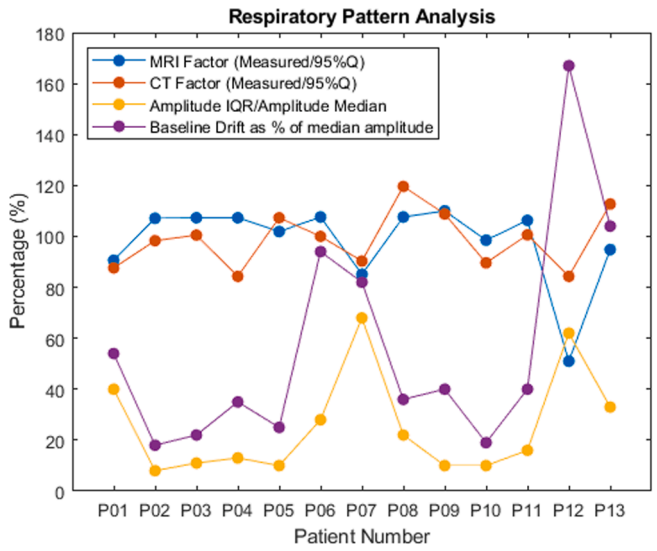

Fig. 2. Visualisation of the amplitude variability and baseline drifts magnitudes compared to the MRI factor and the CT factor. When MRI and CT factor are 100%, the modality is representing the entire 95% quantiles of the actual motion. Baseline Drift is reported as a % of the median amplitude and the Amplitude variability is reported as the interquartile range (equivalent to 1 standard deviation) over the Median Amplitude as a %.

Table 1
Normality test for the motion range distributions of 4D-CT, 4D-MRI and the input respiratory 95% quantiles. High test statistic and p greater than 0.05 suggest normal distributions.

Motion range distribution	Shapiro-wilk (p-value)	Kolmogorov-Smirnov (p-value)
4D-CT	0.98 (0.99)	0.42 (0.99)
Input Respiratory (Q95%)	0.91 (0.20)	0.67 (0.76)
4D-MRI	0.90 (0.12)	0.71 (0.70)

4. Discussion

In the evaluation of 4D-MRI radial VIBE with self-navigation for use in lung cancer radiotherapy treatment planning, we compared motion range detection capability with conventional 4D-CT in a phantom model. The results of this study showed that the difference between the motion range detection capability of 4D-CT and 4D-MRI was not statistically significant when using 13 patient respiratory traces to generate pseudo-realistic phantom motion. While the use of MRI for detection, staging and surveillance of early stage lung cancer is well established [16], with recent developments in MR-guided radiotherapy [17–20], MRI simulators and the move toward MRI only workflows, results such as those reported in this study, which show equivalence between MRI and CT techniques, may be particularly relevant.

The high Spearman's Rank Correlation (close to 1) for all 4D-CT RPM signal trace data measured in this study, reduces the likelihood of the RPM mechanical device attachment being a confounding parameter as the RPM signal trace was a faithful representation of the input signal trace. The self-navigation signal was found to have a high Spearman's Rank correlation with the input respiratory trace for 12 out of the 13 patients suggesting a large FOV may be adequate for most 4D-MRI use. The self-navigation signal with a low Spearman's correlation (patient 12) had a low median respiratory amplitude and high baseline drift indicative of respiratory distress. Reducing the FOV increased the relative signal change within the imaging volume, leading to significant improvement in respiratory detection as shown in Fig. 1. The increase in response may be helpful for shallow or irregular breathing patients in generating a self-navigating signal that more faithfully represents the motion of the tumour. Depending on the position of the tumour in the lung and its associated respiratory motion, a reduction in FOV may not always increase the proportion of moving tissue within the image. In some cases, this reduction in FOV may have a negative effect on self-navigation performance. Careful consideration should be used when deciding on FOV selection in patients, with tumour location, motion amplitude and proximity to surrounding tissue likely to affect the accuracy of the measured navigation signal.

4D-CT by contrast, has its own limitations; one of which is the dependency on the regularity of breathing for accurate phase binning of image data. If breathing is too irregular, the appropriate phase images are not acquired during all slices, resulting in artefacts and misrepresentation of motion.

The input respiratory signal (Q95%), 4D-MRI and 4D-CT Shapiro-Wilk and Kolmogorov-Smirnov statistics all suggest a normal distribution of data for the measured ranges of motion and ANOVA was therefore indicated as a valid test. The motion ranges detected by 4D-MRI and 4D-CT showed no statistically significant difference between the 4D-MRI, 4D-CT and the 95% quantiles of the input respiratory traces as indicated by the ANOVA small F-statistic/high p-value and paired *t*-test where the p-values are high ($p \gg 0.05$, fail to reject null-hypothesis of no difference between means) which was consistent with Oar et al. [21] abdominal study. In contrast, the report from Steiner, Shieh [12] showed that there was a statistically significant difference between the detected motion ranges for patients between the Calypso radiotracer system (analogous to the input respiratory signal) and 4D-CT and 4D-CBCT. The results of this study has shown that the average 4D-MRI motion range was 96.5% of the average input motion range and the average 4D-CT was 97.4% of the average input motion range. As there was <1% difference between the means of the motion ranges detected and <4% difference to the average input signal, significantly more data would be required to determine the likelihood (if any) of there being a statistically significant difference.

The prototype radial VIBE 4D-MRI sequence performs amplitude-based binning from end exhale to end inhale, with the total number of radial readout 'spokes' divided equally among the specified number of phase bins. Although all measured data is used, the sequence does not distinguish between inspiration and expiration, and therefore cannot visualize hysteresis. This strategy benefits from a symmetrical respiratory cycle which would require the tumour motion to follow the same trajectory in both inspiration and expiration. This is not always the case with lung cancer and is dependent, among other things on the location of the tumour within the lung [22]. Future work will include a detailed investigation into the impact of hysteresis on 4D-MRI measurements and the potential implications for treatment planning.

The small (<1%) difference observed between the means of the detected motion ranges with 4D-CT and 4D-MRI in this study may represent a best-case scenario. A larger discrepancy may occur between the two imaging modalities when applied in lung cancer patients, depending on tumour size, location and motion range, as demonstrated by Borm et al. [2] in their 4D-CT, MIP and AIP comparative study.

With the introduction of motion correction averaging to further improve the imaging performance of MRI through post processing [23,24], as well as superior soft tissue contrast compared to CT, the radial VIBE sequence should be considered for further investigation in patient studies.

In conclusion, this phantom study showed that the 4D-MRI radial VIBE with self-navigation has equivalent motion range detection capabilities for lung tumour delineation as compared to the existing 4D-CT techniques currently used in the clinic.

Declaration of Competing Interest

The authors declare that they have no known competing financial interests or personal relationships that could have appeared to influence

the work reported in this paper.

Acknowledgements

This paper is part of a special issue that contains contributions originally submitted to the scientific meeting MR in RT, which was planned to take place 05/2020, organized by the German Research Center (DKFZ) in Heidelberg. We acknowledge funding by DKFZ for the publication costs of this special issue.

References

[1] Bradley JD, Paulus R, Komaki R, Masters G, Blumenschein G, Schild S, et al. Standard-dose versus high-dose conformal radiotherapy with concurrent and consolidation carboplatin plus paclitaxel with or without cetuximab for patients with stage IIIA or IIIB non-small-cell lung cancer (RTOG 0617): a randomised, two-by-two factorial phase 3 study. Lancet Oncol 2015;16(2):187–99. https://doi.org/10.1016/S1470-2045(14)71207-0.

[2] Borm KJ, Oechsner M, Wiegandt M, Hofmeister A, Combs SE, Duma MN. Moving targets in 4D-CTs versus MIP and AIP: comparison of patients data to phantom data. BMC Cancer 2018;18(1). https://doi.org/10.1186/s12885-018-4647-4.

[3] Werner R, Hofmann C, Mücke E, Gauer T. Reduction of breathing irregularity-related motion artifacts in low-pitch spiral 4D CT by optimized projection binning. Radiat Oncol 2017;12(1). https://doi.org/10.1186/s13014-017-0835-7.

[4] Pollock S, Kipritidis J, Lee D, Bernatowicz K, Keall P. The impact of breathing guidance and prospective gating during thoracic 4DCT imaging: an XCAT study utilizing lung cancer patient motion. Phys Med Biol 2016;61(17):6485–501. https://doi.org/10.1088/0031-9155/61/17/6485.

[5] Brandner ED, Chetty IJ, Giaddui TG, Xiao Y, Huq MS. Motion management strategies and technical issues associated with stereotactic body radiotherapy of thoracic and upper abdominal tumors: A review from NRG oncology. Med Phys 2017;44(6):2595–612. https://doi.org/10.1002/mp.12227.

[6] Chandarana H, Wang H, Tijssen RHN, Das IJ. Emerging role of MRI in radiation therapy: emerging role of MRI in radiation therapy. J Magn Reson Imag 2018;48(6):1468–78. https://doi.org/10.1002/jmri.26271.

[7] Kolbitsch C, Ahlman MA, Davies-Venn C, Evers R, Hansen M, Peressutti D, et al. Cardiac and respiratory motion correction for simultaneous cardiac PET/MR. J Nucl Med 2017;58(5):846–52. https://doi.org/10.2967/jnumed.115.171728.

[8] Robson PM, Trivieri M, Karakatsanis NA, Padilla M, Abgral R, Dweck MR, et al. Correction of respiratory and cardiac motion in cardiac PET/MR using MR-based motion modeling. Phys Med Biol. 2018;63(22):225011-225011, https://doi.org/10.1088/1361-6560/aaea97.

[9] Deng Z, Pang J, Lao Yi, Bi X, Wang G, Chen Y, et al. A post-processing method based on interphase motion correction and averaging to improve image quality of 4D magnetic resonance imaging: a clinical feasibility study. BJR 2019;92(1095):20180424. https://doi.org/10.1259/bjr.20180424.

[10] Deng Z, Pang J, Yang W, Yue Y, Sharif B, Tuli R, et al. Four-dimensional MRI using three-dimensional radial sampling with respiratory self-gating to characterize temporal phase-resolved respiratory motion in the abdomen: characterization of Respiratory Motion. Magn Reson Med 2016;75(4):1574–85. https://doi.org/10.1002/mrm.25753.

[11] Lee D, Greer PB, Ludbrook J, Arm J, Hunter P, Pollock S, et al. Audiovisual biofeedback improves cine–magnetic resonance imaging measured lung tumor motion consistency. Int J Radiat Oncol Biol Phys 2016;94(3):628–36. https://doi.org/10.1016/j.ijrobp.2015.11.017.

[12] Steiner E, Shieh C-C, Caillet V, Booth J, O'Brien R, Briggs A, et al. Both four-dimensional computed tomography and four-dimensional cone beam computed tomography under-predict lung target motion during radiotherapy. Radiother Oncol 2019;135:65–73. https://doi.org/10.1016/j.radonc.2019.02.019.

[13] Yoganathan SA, Maria Das KJ, Agarwal A, Kumar S. Magnitude, impact, and management of respiration-induced target motion in radiotherapy treatment: a comprehensive review. J Med Phys 2017;42(3):101–15. https://doi.org/10.4103/jmp.JMP_22_17.

[14] Grimm R. Reconstruction Techniques for Dynamic Radial MRI. The Technical Faculty of Friedrich-Alexander-University, Erlangen-Nuremberg; 2015.

[15] RStudioTeam, RStudio: Integrated Development Environment for R, I. RStudio, Editor; 2018.

[16] Sim AJ, Kaza E, Singer L, Rosenberg SA. A review of the role of MRI in diagnosis and treatment of early stage lung cancer. Clin Transl Radiat Oncol 2020;24:16–22. https://doi.org/10.1016/j.ctro.2020.06.002.

[17] Stark LS, Andratschke N, Baumgartl M, Bogowicz M, Chamberlain M, Dal Bello R, et al. Dosimetric and geometric end-to-end accuracy of a magnetic resonance guided linear accelerator. Phys Imag Radiat Oncol 2020;16:109–12. https://doi.org/10.1016/j.phro.2020.09.013.

[18] Finazzi T, van Sörnsen de Koste JR, Palacios MA, Spoelstra FOB, Slotman BJ, Haasbeek CJA, et al. Delivery of magnetic resonance-guided single-fraction stereotactic lung radiotherapy. Phys Imag Radiat Oncol 2020;14:17–23. https://doi.org/10.1016/j.phro.2020.05.002.

[19] Eccles CL, Adair Smith G, Bower L, Hafeez S, Herbert T, Hunt A, et al. Magnetic resonance imaging sequence evaluation of an MR Linac system; early clinical experience. Techn Innov Patient Supp Radiat Oncol 2019;12:56–63. https://doi.org/10.1016/j.tipsro.2019.11.004.

[20] Tetar SU, Bruynzeel AME, Lagerwaard FJ, Slotman BJ, Bohoudi O, Palacios MA. Clinical implementation of magnetic resonance imaging guided adaptive radiotherapy for localized prostate cancer. Phys Imag Radiat Oncol 2019;9:69–76. https://doi.org/10.1016/j.phro.2019.02.002.

[21] Oar A, Liney G, Rai R, Deshpande S, Pan Li, Johnston M, et al. Comparison of four dimensional computed tomography and magnetic resonance imaging in abdominal radiotherapy planning. Phys Imag Radiat Oncol 2018;7:70–5. https://doi.org/10.1016/j.phro.2018.09.004.

[22] White B, Zhao T, Lamb J, Wuenschel S, Bradley J, El Naqa I, et al. Distribution of lung tissue hysteresis during free breathing: distribution of lung tissue hysteresis during free breathing. Med Phys 2013;40(4):043501. https://doi.org/10.1118/1.4794504.

[23] Bi X, Pang J, Wensha Y, Fenchel M, Deng Z, Chen Y, et al., Improving Respiratory Phase-resolved 3D Body Imaging Using Iterative Motion Correction and Average (MoCoAve). Proc Intl Soc Mag Reson Med 24. 2016, ISMRM: Singapore.

[24] Gratz M, Ruhlmann V, Umutlu L, Fenchel M, Hong I, Quick HH. Impact of respiratory motion correction on lesion visibility and quantification in thoracic PET/MR imaging. PLoS One. 2020;15(6):e0233209-e0233209, https://doi.org/10.1371/journal.pone.0233209.